Journal of Intelligent & Robotic Systems (2019) 94:405–421
https://doi.org/10.1007/s10846-018-0935-0

Analysis and Design of a Time-Varying Extended State Observer for a Class of Nonlinear Systems with Unknown Dynamics Using Spectral Lyapunov Function

Mehran Attar[1] · **Vahid Johari Majd**[1] · **Navid Dini**[1]

Received: 27 December 2017 / Accepted: 24 September 2018 / Published online: 25 October 2018

Abstract

In this study, a novel strategy based on the integration of differential algebraic spectral theory (DAST) and spectral Lyapunov function is presented to analyze and design a time-varying extended state observer (TESO) for a class of nonlinear systems with unknown dynamics. The simultaneous estimation of the lumped disturbance and state vectors are achieved by using a TESO based on the time-varying parallel differential (PD) eigenvalues of the observer. The observer bandwidth design is based on the combination of DAST and spectral Lyapunov function. By using this method, a systematic approach is derived to obtain the observer parameters, which improves boundedness of the observer estimation error in terms of transient and persistent performance. A comparison between TESO and previous similar methods is provided in the simulation part upon the TMUBOT quadruped robot dynamic model which indicates a distinguished answer in the estimation error of the TESO. Moreover, by applying the proposed algorithm to the TMUBOT robot, the superiority of the algorithm in practical schemes will be illustrated.

Keywords Active disturbance rejection control · Extended state observer · Differential algebraic spectral theory · Spectral Lyapunov function

1 Introduction

Disturbances and uncertainties occur in many industrial systems in the form of external disturbances and unknown dynamics. Control of such systems is usually associated with difficulties and high costs in hardware implementation and has become a cardinal interest for researchers in recent decades. A solution introduced to this problem is the use of disturbance observers as a powerful tool for estimation and compensation of various disturbances which also improves the control performance, and has been deeply discussed in the literature [1–4]. Another way of disturbance estimation is the use of extended state observers (ESO's) [5–7], for active disturbance rejection. In this method, all of the internal and external disturbances are considered as a lumped disturbance state, and then the extended state vector of the augmented system is estimated. Due to its' advantages, including ease of analysis and design and also great efficiency, this method has been used in different industries, such as robotics, aerospace, electrical machines and so on. [8–11]. In early works linear ESO (LESO) was used for estimation and compensation of the disturbances in systems. This method provides easy analysis and simplicity of parameter tuning [12–14]. Moreover, when an extended state observer based control structure (The ADRC approach) is used, the tracking error will be more decreased than some classic control structures, like PID controller. This issue has been investigated in many studies [15, 16]. Also, [17], has presented a practical verification of an extended state observer based PD controller method in governing a multidimensional system which ADRC robustness experimentally has compared with the

✉ Vahid Johari Majd
majd@modares.ac.ir
http://www.modares.ac.ir/~majd

Mehran Attar
mehran.attar@modares.ac.ir

Navid Dini
navid.dini@modares.ac.ir

[1] Intelligent Control Systems Laboratory, School of Electrical and Computer Engineering, Tarbiat Modares University, P.O. Box 14115-194, Tehran, Iran

results obtained from using a classic PID controller and significantly better results, in terms of parametric robustness, have been reported for the ADRC approach. However, the linear structure of the LESO may not be appropriate for complicated systems, due to its loss of design flexibility [18, Ch.14]. Additionally, LESO may require large observer gains to have an acceptable performance, which may cause large control signals and even peaking phenomenon may appear in the case of large gains and as a result, it is inappropriate for practical schemes [19]. Nonlinear ESO (NESO) is another class of these observers. Due to their nonlinear structures, NESO yields a better efficiency in the estimation of variables (lumped disturbance and state vectors), compared to LESO. However, because of its sophisticated nonlinear structure, rigorous stability derivation for NESO is difficult to be carried out. Also, the nonlinear structure needs more conservative conditions in the design process, which may be physically infeasible [20]. The convergence analysis of the NESO has been discussed in [21], for SISO systems, and in [22] for MIMO systems. It is desirable to design an observer that can benefit from the advantages of both LESO's and NESO's to overcome the aforementioned difficulties, to derive a proper simultaneous estimation of disturbances and states of the system. Hence, time-varying extended state observers (TESO's), as a new class of ESO, has been introduced in [23], which in particular could have a linear structure with time-varying parameters. Boundedness of the estimation error dynamic of TESO was investigated based on the theorems of LTV systems, such as Floquent factorization, and differential algebraic spectral theory [24–27]. Nevertheless, this work has not provided any solutions on how to analyze and design the observer's time-varying parameters.

In this paper, by analyzing the convergence of the observer estimation error using DAST and spectral Lyapunov function, the relationship between observer's bandwidth and parameters of the estimation error envelope has been acquired. As a result, a systematic procedure for appropriate designing of the observer bandwidth and PD eigenvalues will be determined to improve performance in the transient and persistent response of the observer estimation error. In other words, by assigning a proper time-varying PD spectrum not only the uniform ultimate boundedness of the estimation error is guaranteed, but also a proper flexibility in designing of the observer parameters will be attained, which make it applicable to use in practical applications. Verification of the proposed method through simulation and implementation on the TMUBOT quadruped robot in the motion scenario has been investigated. Quadruped robot is a system with a complicated dynamic equation which includes internal and external disturbances [28] and the experiment was performed with only partial knowledge about the mathematical model of the plant.

The paper is organized as follows. Section 2 briefly introduces the TESO structure and DAST. In Section 3, necessary theorems for the convergence analysis of TESO and its parameter design are provided. Necessary conditions for convergence and also modifications for a better estimation performance have been introduced in this section. Section 4, which includes two parts, verifies the ability of the presented method through evaluating the results in simulation and implementation on the TMUBOT robot. Section 5 includes conclusions which have been obtained via this paper and future works.

2 The Problem Statement and Preliminaries

Consider the following n-dimensional nonlinear system, i.e.,

$$y^{(n)}(t) = f\left(y^{(n-1)}(t), \ldots, y(t), w(t)\right) + b_0 u(t), \quad (1)$$

Where $u(t)$ and $y(t)$ are the system input, and output, respectively,b_0 is a known constant, $w(t)$ is the external disturbance, and the unknown function $f(.)$ represents the nonlinear dynamics of the system, which could include uncertainties and considered as the total disturbance. System (1) is used as a mathematical model for a large variety of practical systems. It is assumed that $f(.)$ is locally Lipschitz and differentiable with the derivative of the form:

$$\dot{f} = h\left(y^{(n-1)}(t), \ldots, y(t), w(t)\right), \quad (2)$$

where h is assumed to be an unknown, but bounded function. In order to tackle the problem regarding the lack of other information about the system, a time-varying extended state observer (TESO) will be used to estimate the unknown function $f(.)$. Equation 1 can be rewritten in the extended state spaceform, i.e.,

$$\begin{cases} \dot{x}_1 = x_2 \\ \vdots \\ \dot{x}_{n-1} = x_n \\ \dot{x}_n = x_{n+1} + b_0 u \\ \dot{x}_{n+1} = h(x, w) \\ y = x_1 \end{cases}, \quad (3)$$

where $y = x_1$ and $x = [x_1, \ldots, x_{n+1}]^T$. Equation 3 is called the extended form of system (1), since the total disturbance, f is considered as a new state of the system, x_{n+1}. The general form of the TESO can be written in the following form [23]:

$$\begin{cases} \dot{\hat{x}}_1(t) = \hat{x}_2(t) - l_1(t)\left(\hat{x}_1(t) - y(t)\right) \\ \dot{\hat{x}}_2(t) = \hat{x}_3(t) - l_2(t)\left(\hat{x}_1(t) - y(t)\right) \\ \vdots \\ \dot{\hat{x}}_n(t) = \hat{x}_{n+1}(t) - l_n(t)\left(\hat{x}_1(t) - y(t)\right) + b_0 u(t) \\ \dot{\hat{x}}_{n+1} = -l_{n+1}(t)\left(\hat{x}_1(t) - y(t)\right) \end{cases}, \quad (4)$$

Here $\hat{x}_i(t), i = 1,\ldots,n+1$, is the estimated value of x_i and $l_i(t), i = 1,\ldots,n+1$, is the observer gain to be designed. By subtracting Eq.(3) from Eq.(4), the error dynamic equation of TESO will be obtained as:

$$\begin{cases} \dot{e}_1 = e_2 - l_1(t)\, e_1 \\ \vdots \\ \dot{e}_{n-1} = e_n - l_{n-1}(t)\, e_1 \\ \dot{e}_n = e_{n+1} - l_n(t)\, e_1 \\ \dot{e}_{n+1} = -l_{n+1}(t)\, e_1 - h(x,w) \end{cases} . \tag{5}$$

Where $e_i(t) = \hat{x}_i(t) - x_i(t)$ and $e = \left[e_1 \ldots . e_{n+1}\right]^T$. Equation 5 can be rewritten in the following matrix form:

$$\dot{e} = A(t)\, e + b\left(-h(x.w)\right), \tag{6}$$

Where

$$A(t) = \begin{bmatrix} -l_1(t) & 1 & 0 & 0 & 0 \\ -l_2(t) & 0 & 1 & \ldots & 0 \\ \vdots & \vdots & \ddots & \ddots & \vdots \\ -l_n(t) & 0 & \ldots & 0 & 1 \\ -l_{n+1}(t) & 0 & 0 & 0 & 0 \end{bmatrix}, b = \begin{bmatrix} 0 \\ 0 \\ \vdots \\ 0 \\ 1 \end{bmatrix}$$

Equation 6 shows a linear time-varying system, perturbed with unknown but bounded dynamic as follows:

$$\|b(-h(x.w))\| \leq \delta \tag{7}$$

On the other hand, Eq. 6 is a canonical form of LTV systems that are uniformly controllable [29]. The perturbed term is nonvanishing in general, thus the origin is not necessarily an equilibrium point of the perturbed system (6) and therefore, in this case, ultimate boundedness of the solutions of the perturbed system is studied [18]. The main problem is to find $l_i(t)$ such that the ultimate boundedness of the estimation error dynamics is guaranteed. For this purpose, first, the stability analysis of the homogeneous form of Eq. 6, as a nominal system is expressed and according to the gained results, the relationships between PD eigenvalues and the parameters of the estimation error upper bound of TESO will be determined. In fact, these relationships will be achieved by using DAST and spectral Lyapunov function. Then, a systematic approach has been provided for the joint estimation of states and disturbances and it will be shown that, how the designer can decrease amplitude, increase convergence and keep the final value of the estimation error upper bound of the TESO in Eq. 4 in order to improve the performance of the estimation error. Finally, the results will be extended to the non-homogeneous system (6) and it will be illustrated that how the observer bandwidth affects the estimation error upper bound parameters. Before doing so, it is necessary to transform (6) into the canonical phase variable format. This will be discussed in the next subsection.

2.1 Canonical Transformation of the TESO Error Dynamics Equations

Due to the fact that phase variable canonical form is used in DAST, first, Eq. 6 should convert to this form. For this purpose, the presented results in [27], have been used. Finally, a comprehensive analysis of the stability and estimate error bounds of the proposed TESO (4) will be conducted. The phase variable canonical form of Eq. 6 is as follows:

$$\dot{z} = A_c(t)\, z + b_c\left(-h(x,w)\right),$$

$$A_c(t) = \begin{bmatrix} 0 & 1 & 0 & \ldots & 0 \\ 0 & 0 & 1 & \ldots & 0 \\ \vdots & \vdots & \ddots & \ddots & \vdots \\ 0 & 0 & \cdots & 0 & 1 \\ a_1(t) & a_2(t) & \cdots & a_n(t) & a_{n+1}(t) \end{bmatrix}, b_c = \begin{bmatrix} 0 \\ 0 \\ \vdots \\ 0 \\ 1 \end{bmatrix}. \tag{8}$$

where $a_i(t)$ is assumed to be continuous, differentiable of order n and bounded. Let $z = T(t)\, e$, where the transformation matrix $T(t)$ is defined as follows [30]:

$$T(t) = M_{cz}(t) M_{c_e}^{-1}(t). \tag{9}$$

In the above equation M_{c_e} and M_{cz} are the controllability matrices of the LTV system (6) and (8), respectively.

Definition 1 [27] Matrix $T(t)$, is said to be Lyapunov transformation matrix if:

i) $T(t)$ and $\dot{T}(t)$, are continuous.
ii) $T(t)$ is nonsingular.
iii) $\|T(t)\|$, and $\left\|T^{-1}(t)\right\|$ are bounded.

Regarding the fact that $a_i(t)$ is continuous, differentiable and bounded, $T(t)$ is considered as a Lyapunov transformation. If $T(t)$ is a Lyapunov transformation matrix, then the following relationships are established:

$$A(t) = T^{-1}(t)\left(A_z(t)\, T(t) - \dot{T}(t)\right), \tag{10}$$

$$b = T^{-1}(t)\, b_c \tag{11}$$

To obtain the observer gain, $l_i(t)$ in Eq. 6 through the element $a_i(t)$ in Eq. 7, define the vector of observer parameters, i.e.,

$$L(t) = \left[-l_1(t) \ldots -l_{n+1}(t)\right]^T, \tag{12}$$

And divide $T(t)$ into $n+1$ columns as

$$T(t) = \left[-T_1(t) \ldots -T_{n+1}(t)\right]^T \tag{13}$$

where the column vector $T_i(t) \in R^{n+1}, i = 1, 2, \ldots, n+1$. Based on Eq. 10, the vector of observer parameters is calculated as:

$$L(t) = T^{-1}(t)\left(A_z(t)\, T_1(t) - \dot{T}_1(t)\right) \tag{14}$$

According to Eq. 14, it was shown that how $l_i(t)$ can be written based on $a_i(t)$. For instance, for a second order system with a third order extended state observer, the following results obtain:

$$T = (t)\begin{bmatrix} 1 & 0 & 0 \\ -a_3(t) & 1 & 0 \\ \dot{a}_3(t) + a_3^2(t) - a_2(t) & -a_3(t) & 1 \end{bmatrix}, \tag{15}$$

$$\begin{cases} l_1(t) = a_3(t) \\ l_2(t) = a_2(t) - 2\dot{a}_3(t) \\ l_3(t) = a_1(t) + \ddot{a}_3(t) - \dot{a}_2(t) \end{cases}. \tag{16}$$

2.2 Overview of the DAST [26]

DAST for LTV systems is a generalization of algebraic spectral theory of LTI systems. The PD eigenvalues that have defined in DAST are different from the frozen time eigenvalues calculated as follows:

$$\dot{x} = Ax(t), \det(I\lambda(t) - A(t)) \tag{17}$$

Consider the following LTV system:

$$\dot{z} = A_z(t)\, z, z(t_0) = z_0, \quad t \geq t_0 \tag{18}$$

Where $A_z(t)$ is a continuous, bounded matrix, defined as:

$$A_z(t) = \begin{bmatrix} 0 & & \\ \vdots & & I_{n-1} \\ 0 & & \\ -a_1(t) & -a_2(t) & \cdots & -a_n(t) \end{bmatrix}. \tag{19}$$

If it is assumed that $y = z_1$, then the corresponding time-varying differential equation is as follows:

$$y^n + \alpha_n(t)\, y^{n-1} + \ldots + \alpha_2(t)\, \dot{y} + \alpha_1(t)\, y = 0 \tag{20}$$

The general solution to Eq. 20 is:

$$y(t) = \sum_{k=1}^{n} c_k e^{\int_{t0}^{t} \rho_k(\tau) d\tau} \tag{21}$$

Where the set $\{\rho_k(t)\}_{k=1}^{n}$ is a parallel differential (PD) spectrum of Eq. 20, and $\rho_k(t)$ are PD eigenvalues of $A_z(t)$. The PD characteristic equation of Eq. 18 is:

$$\begin{aligned} \Delta(\rho) &= D_\rho^{n-1}(\rho) + \alpha_n(t) D_\rho^{n-2}(\rho) + \ldots + \alpha_3(t) D_\rho(\rho) + \alpha_2(t)\rho + \alpha_1(t) = 0 \\ D_\rho(\rho) &= \left[\frac{d}{dt} + \rho(t)\right]\rho(t), D_\rho^k = D_\rho D_\rho^{k-1}. \end{aligned} \tag{22}$$

The solutions of Eq. 22 are the PD eigenvalues of Eq. 18. Also, there exists an eigenvector $\mu_i(t)$ for each of the PD eigenvalues $\rho_i(t)$, which satisfy the following equation:

$$A_z(t)\, \mu_i(t) - \rho_i(t)\, \mu_i(t) = \dot{\mu}_i(t) \tag{23}$$

Where $\mu_i(t)$ is defined as:

$$\mu_i(t) = [1 D_{\rho_i}(1)\, D_{\rho_i}^2(1) \ldots D_{\rho_i}^{n-1}(1)]^T \tag{24}$$

The diagonal matrix of $\rho_i(t)$ is defined as follows:

$$\psi(t) = diag[\rho_1(t), \rho_2(t), \ldots, \rho_n(t)] \tag{25}$$

where, $\psi(t)$ is the PD spectral canonical form of $A_z(t)$. The PD modal matrix for $A_z(t)$ is defined as follows:

$$M(t) = [\mu_1(t)\, \mu_2(t) \ldots \mu_n(t)] \tag{26}$$

A PD spectrum, such as $\{\rho_k(t)\}_{k=1}^{n}$ is said to be well-defined, if all of its PD eigenvalues are bounded, continuous and differentiable of order n.

Definition 2 The PD modal matrix is called diffeomorphism if:

i) it is continuous and differentiable.
ii) its inverse is continuous and differentiable.

If a bounded PD modal matrix is diffeomorphism then it would be a Lyapunov transformation matrix. The following equation can be used to derive the PD spectral canonical form of $A_z(t)$:

$$\psi(t) = M^{-1}(t)\left[A_z(t)\, M(t) - \dot{M}(t)\right] \tag{27}$$

In this paper, the required Lyapunov candidates for investigating the exponential stability of Eq. 8 are derived based on the PD modal matrix and this Lyapunov function is called Spectral Lyapunov function. Then, a design procedure for the PD eigenvalues and time shaping of the time-varying observer bandwidth is derived and accordingly, by shaping the observer bandwidth, the observer estimation error will be improved. If $z = 0$ is the stable exponential equilibrium point for Eq. 18, then there exists a Lyapunov function as follows:

$$V_z(t, z) = z^*(t)\, P_z(t)\, z(t) \tag{28}$$

with its time derivative as:

$$\dot{V}_z(t, z) = -z^*(t)\, Q_z(t)\, z(t) \tag{29}$$

In Eqs. 28 and 29, $P_z(t)$ and $Q_z(t)$ are positive definite matrices for all $t > 0$ and have the following relation [26]:

$$P_z(t) = \int_t^\infty \varphi_z^*(\tau, t)\, Q_z(\tau)\, \varphi_z(\tau, t)\, d\tau \tag{30}$$

where $\varphi_z(\tau, t)$ is the state transition matrix for the system (18). In the above equations * means the transpose conjugate. The following lemma provides the transformed Lyapunov matrices under Lyapunov transformation of an

original stable system. According to lemma1, the stability of a system is retained under Lyapunov transformation. Lemma1 will be used to verify the stability of Eqs. 6 and 8, that are linked through a Lyapunov transformation.

Lemma 1 [26] *For the exponentially stable system (18), with Lyapunov transformation matrix $M(t)$, using state transformation:*

$$x(t) = M(t)\, z(t) \tag{31}$$

then, the transformed system is as follows:

$$\dot{x} = A_x(t)\, x \tag{32}$$

and $x = 0$ is the exponentially stable equilibrium of Eq. 32, where:

$$A_x(t) = M^{-1}(t)\, A_z(t)\, M(t) - M^{-1}(t)\dot{M}(t) \tag{33}$$

and there exists a Lyapunov function $V_x(t,x) = x^*(t)\, P_x(t)\, x(t)$, with time derivative $\dot{V}_x(t,x) = -x^*(t)\, Q_x(t)\, x(t)$, where $P_x(t) > 0$ and $Q_x(t) > 0$ are given by:

$$P_x(t) = M^{*-1}(t)\, P_z(t)\, M^{-1}(t) \tag{34}$$

$$Q_x(t) = M^{*-1}(t)\, Q_z(t)\, M^{-1}(t) \tag{35}$$

3 Stability and Estimate Error Bound Analysis of TESO

In this section, theorems on the boundedness of TESO estimation error using spectral Lyapunov function will be examined. According to Eq. 6, the TESO estimation error is an LTV perturbed system. First, Theorem 1 for the homogeneous form of TESO estimation error will be presented and derive some conclusions on how to design the PD eigenvalues or bandwidth of TESO. Then, the relationship of TESO's PD eigenvalues with the estimation error upper bound parameters of TESO is determined. Using these results, the time shaping of the observer bandwidth to provide a better estimation is investigated. Based on the mentioned points, the stability analysis of the homogeneous form of system (6), will be explored based on the spectral Lyapunov function. The presented theorem and the design method will then be generalized for the case of the non-homogeneous dynamical error equation (6), through Theorem 2.

Theorem 1 *Let $\psi(t)$, be a well-defined PD spectral matrix for the homogeneous form of Eq. 8, and $M(t)$ be the corresponding bounded and diffeomorphism PD modal matrix given in Eq. 26. If $Re(\rho_k(t)) < 0$, then the homogeneous form of Eq. 8 is exponentially stable and there exists a Lyapunov function $V_z(t,z) = z^*(t)\, P_z(t)\, z(t)$, with time derivative $\dot{V}_z(t,z) = -z^*(t)\, Q_z(t)\, z(t)$, where $P_z(t) > 0$ and $Q_z(t) > 0$ are the Lyapunov matrices for examining the stability of homogeneous form of Eq. 8, and are as follows:*

$$P_z(t) = M^{*^{-1}}(t)\, M^{-1}(t),$$

$$Q_z(t) = -2M^{*^{-1}}(t)\, Re(\psi(t))\, M^{-1}(t) \tag{36}$$

Proof If $\psi(t)$ satisfies $Re(\rho_k(t)) < 0, k = 1, \ldots, n$, and define $\varepsilon(t) = M^{-1}(t)\, z(t)$, since $M(t)$ is a Lyapunov transformation, therefore the transformation will not change the stability of the system [Lemma 1]. According to Eq. 27, the modal form of homogenous system (8), will beobtained as follows:

$$\dot{\varepsilon} = \psi(t)\, \varepsilon \tag{37}$$

If $V_\varepsilon(t,\varepsilon) = \varepsilon^*(t)\, P_\varepsilon(t)\varepsilon(t)$, $P_\varepsilon(t) = I$, is a Lyapunov function for Eq. 37 then its time derivative along the trajectories is:

$$\dot{V}_\varepsilon(t,\varepsilon) = 2\varepsilon^*(t)\, Re(\psi(t))\, \varepsilon(t) \tag{38}$$

It is obvious that $\dot{V}_\varepsilon(t,\varepsilon) < 0$, due to the fact that $Re(\psi(t)) < 0$. Therefore, $\varepsilon = 0$ is the exponentially stable equilibrium for Eq. 37. Using (34) and (35), The Lyapunov matrices related to the Lyapunov function, that proves the exponential stability of homogenous form of Eq. 8, are then derived from Eq. 36. Finally, because (8) was derived by the application of the Lyapunov transformation, $T(t)$ on Eq. 6, it can be concluded that $e = 0$ is the exponentially stable equilibrium of the homogenous form of Eq. 6. □

Remark 1 According to theorem1, only negative PD eigenvalues should be considered in the design process. In other words, theorem1, not only proves the stability of the homogeneous dynamical error equation (6), but also provides a relationship between the PD modal matrix $M(t)$ and observer parameters in order to improve TESO estimation performance.

Remark 2 According to [18, Theorem 4-12], the following upper bound for TESO estimation error is established:

$$\|e(t)\| \leq \kappa\, \|e(t_0)\|\, e^{-\mu(t-t_0)} \tag{39}$$

Where

$$\kappa = \sqrt{\frac{c_2}{c_1}}, \mu = \frac{c_3}{2c_2} \tag{40}$$

The coefficients c_1-c_4 are calculated as follows:

$$c_1 = (\lambda_k(P_z(t))), c_2 = (\lambda_k(P_z(t))),$$

$$c_3 = (\lambda_k(Q_z(t))), c_4 = (\lambda_k(Q_z(t))). \tag{41}$$

Where $\lambda_k(X(t))$ denotes the kth algebraic eigenvalue of the time-varying matrix $X(t)$. According to Eqs. 40, 41 and 36, κ and μ depend on$\rho_i(t)$. Also, $\rho_i(t)$ can be considered as a coefficient of the observer bandwidth and a constant eigenvalue. Therefore, by designing proper constant eigenvalues and bandwidth, it is possible to improve the gain and the convergence rate of TESO estimation error upper bound, i.e. a proper bandwidth and constant eigenvalue can decrease the gain and increase the convergence rate of TESO estimation error upper bound resulting in better estimation of internal and external disturbances. Hence, the overall performance of the system besides the controller will increase.

The above results are also applicable for the non-homogeneous system (6). Theorem 2 provides conditions for the boundedness of the non-homogeneous form of system (6) using spectral Lyapunov function. In theorem 2, the results of the [18, Lemma 9.2] have been used.

Theorem 2 *For the LTV perturbed system (6), assume a Lyapunov transformation $z = T(t)e$ that transforms (6) into (8). Also, Consider $\{\rho_k(t)\}_{k=1}^{n}$, is the PD spectrum of Eq. 6 where $\rho_k(t)$ are bounded, continuous, and differentiable. Let $M(t)$ be the corresponding bounded and diffeomorphism PD modal matrix. Also, assume that$(\rho_k(t)) < 0$,and the perturbed term $b(-h(x,w))$, is nonvanishing in the origin which satisfies the following condition:*

$$\|-bh(x,w)\| \leq \delta < \frac{c_3}{c_4}\sqrt{\frac{c_1}{c_2}}\theta r \tag{42}$$

Then, for $t \geq 0$, and $e \in D$, $D = \{e \in R^n \mid \|e\| < r\}$, and $0 < \theta < 1$,with $\|e(t_0)\| < \sqrt{\frac{c_1}{c_2}}r$, $e(t)$ would satisfy the following:

$$\begin{cases} \|e(t)\| < \kappa exp^{-\gamma(t-t_0)}\|e(t_0)\|, & \forall t_0 \leq t \leq t_0+T \\ \|e(t)\| \leq \eta, & \forall t \geq t_0+T. \end{cases} \tag{43}$$

where

$$\kappa = \sqrt{\frac{c_2}{c_1}}, \gamma = \frac{(1-\theta)c_3}{2c_2}, \eta = \frac{c_4}{c_3}\sqrt{\frac{c_2}{c_1}}\frac{\delta}{\theta} \tag{44}$$

The coefficients c_1-c_4 are already defined in Eq. 41.

Proof According to Theorem 1, if $\psi_e(t)$ is the PD spectral matrix for $A(t)$ in Eq. 6, and also condition $Re(\rho_i(t)) < 0$ holds, then the homogenized system (6), will be exponentially stable, and $e = 0$ is the stable equilibrium point of the system. For such a system, a Lyapunov function $v(te)$ is defined as follows:

$$v(t,e) = e^T P(t) e \tag{45}$$

Where$P(t) = M^{*^{-1}}(t) M^{-1}(t)$, satisfies Lyapunov equation, $-\dot{P}(t) = P(t)A(t) + A^T(t)P(t) + Q(t)$. Also, the following conditions hold for the Lyapunov function $v(te)$, [18]:

$$c_1\|e\|^2 \leq v(t,e) \leq c_2\|e\|^2 \tag{46}$$

$$\frac{\partial v}{\partial t} + \frac{\partial v}{\partial e}(A(t)e) \leq -c_3\|e\|^2 \tag{47}$$

$$\left\|\frac{\partial v}{\partial e}\right\| \leq c_4\|e\| \tag{48}$$

By using Eq. 45 and aforementioned conditions, Eqs. 46, 47, 48, for the perturbed system (6), the derivative of $v(t,e)$ along the trajectories satisfies:

$$\begin{aligned} &\dot{v}(t,e) = \dot{e}^T P(t) e + e^T \dot{P}(t) e + e^T P(t)\dot{e} = \\ &-e^T Q(t) e + 2e^T P(t)(b(-h(x,w))) = \\ &-e^T Q(t) + \frac{\partial v(t,e)}{\partial e}(b(-h(x,w))) \leq \\ &-c_3\|e\|^2 + \left\|\frac{\partial v(t,e)}{\partial e}\right\|\|b(-h(x,w))\| \leq -c_3\|e\|^2 + c_4\delta\|e\| \end{aligned} \tag{49}$$

By choosing a proper $0 < \theta < 1$, it can be shown that:

$$\begin{aligned} &\dot{v}(t,e) \leq -(1-\theta)c_3\|e\|^2 - \theta c_3\|e\|^2 + c_4\delta\|e\| \\ &\leq -(1-\theta)c_3\|e\|^2, \forall \|e\| \geq \frac{\delta c_4}{\theta c_3} \end{aligned} \tag{50}$$

Therefore, $v(t,e)$ is a spectral Lyapunov function for Eq. 6 because the Lyapunov matrices are composed of PD modal matrix $M(t)$. Finally, according to [18, lemma 9.2], if Eq. 42 holds, then Eq. 43 can be established. □

Remark 3 It can be concluded from Theorem 2 that TESO estimation error upper bound parameters can be controlled by PD eigenvalues of TESO estimation error or observer bandwidth. In other words, the designer can investigate the effect of the observer bandwidth on each of these parameters and find appropriate values of the observer bandwidth to have the desired performance in the estimation error of the observer response.

In the next part, the proposed algorithm is applied to the TMUBOT Quadruped robot with twelve degrees of freedom, in order to verify the TESO performance in the estimation of unknown dynamics. Also, the process of designing TESO bandwidth is investigated.

4 Experimental Results

To have a proper assessment of the effectiveness of the proposed theory, TMUBOT robot has been used as a real platform (see Fig. 1). Simulation and implementation results of the proposed algorithm on TMUBOT robot have been presented through some real scenarios. TMUBOT has been designed and built in the intelligent control systems

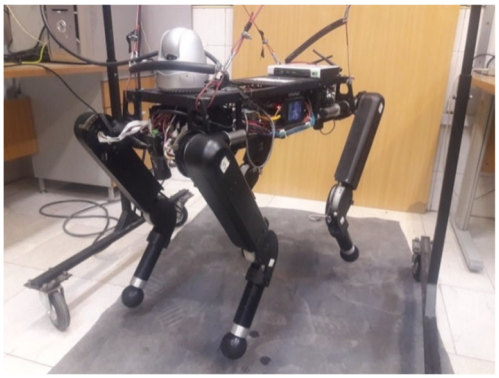

Fig. 1 TMUBOT quadruped robot at ICSLAB

laboratory (ICSLAB) at Tarbiat Modares University and it is a quadruped robot with twelve degrees of freedom (DOF) with each leg of the robot having three DOFs (see Fig. 2). Table 1 shows some physical and mechanical features of the system [31]. Since the considered system is a MIMO system, decentralized structure of the system has been derived and used therefore, the system dynamic equation has converted to SISO sub-systems. Finally, for each sub-system, a TESO has been designed in order to estimate and compensate internal disturbance caused the couplings between the subsystems and also, external disturbance due to the collision of the robot's foot to the ground and the friction force. In the simulation part, a comparison between the performance of TESO and LESO estimation error has been made. Also, in the implementation part, a TESO has been designed for each joint of the robot which compensates the lumped disturbance through

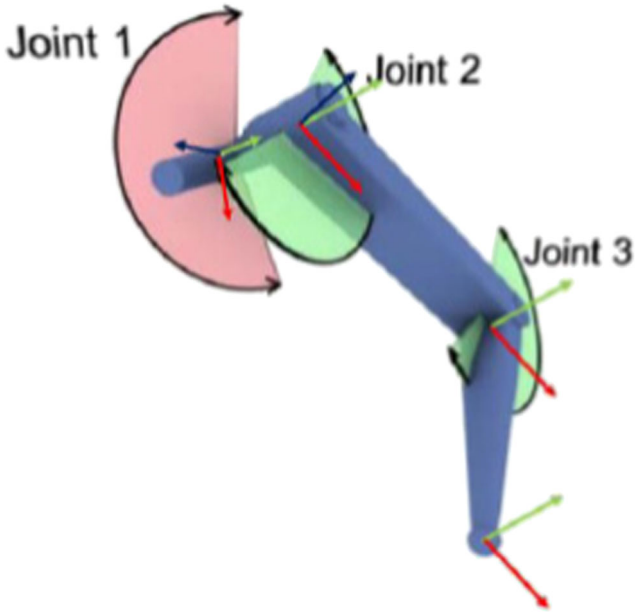

Fig. 2 The leg structure of TMUBOT

a decentralized PD controller (active disturbance rejection structure). The proposed structure has been applied to TMUBOT and the utilized results have been compared with a decentralized PID controller in the same conditions.

4.1 Simulation Results

In this section, the dynamic model of a quadruped walking robot is presented briefly, and then the decentralized dynamic equations of the system are extracted. Therefore, each joint of the robot is considered a sub-system and a TESO and PD controller are designed for each sub-system in order to track the desired gait. The dynamic model of the quadruped robot based on the active joint variables is given by [32]

$$\mathrm{M}\ddot{q} + C\dot{q} + G + D = \tau - \tau_f - J_g^T F_g \tag{51}$$

Where$\mathrm{M} = M(q) + L^T M_o(x_o) L, L = J_o^+(x_o) J_e(q), C = C(q,\dot{q}) + L^T \left(M_o \dot{L} + C_o(x_o,\dot{x}_o) L\right), G = G(q) + L^T G_o(x_o)$ and $D = D$. Equation 51 includes leg and body dynamics, where q is the joint position vector, τ is the vector of joint torques, τ_f is the joint friction, $M(q)$ is the inertia matrix of the leg,$C(q,\dot{q})$ is the vector of leg centrifugal and Coriolis terms, $G(q)$ is the vector of leg gravity terms, D is the vector of leg external disturbances, F_g is the vector of ground reaction forces of the leg. Furthermore, x_o is the position/orientation vector of the body, M_o is the symmetric positive definite inertia matrix of the body, C_o is the Corioli and centrifugal matrix, G_o is the gravitational force vector and J_e, J_g, J_o are the Jacobian matrix from the connect point of the legs to the joint space, Jacobian matrix related to the ground reaction forces, Jacobian matrix from the body to the leg frame respectively [33]. According to Eq. 51, the dynamic equation of active joints of the robot, as a sub-system can be rewritten as follows:

$$\ddot{q}_i(t) = b_i(q)u_i(t) + f_i(q\dot{q}x_o) \tag{52}$$

Where in Eq. 52, $i = 1 \ldots 12$ shows the index of each sub-system or the number of active degrees of freedom of the system, $q = [q_1 \ldots q_{12}]^T$ is the vector of active joint variables, u_i is the joint torque created by the actuators of the system or system inputs, b_i is the system input coefficient and $f_i(q\dot{q}x_o)$ is the dynamic term that consists of all couplings between active and inactive joints. By considering state equations as $x_{i,1}(t) = q_i(t), x_{i,2}(t) = \dot{q}_i(t)$, the general state space form of Eq. 52 is as follows:

$$\begin{cases} \dot{x}_{i,1}(t) = x_{i,2}(t) \\ \dot{x}_{i,2}(t) = f_i(q,\dot{q},x_o) + b_i(q)\,u_i(t) \end{cases}, \tag{53}$$

Where (53), shows iSISO sub-system. The extended state form of Eq. 53, is obtained as follows:

$$\begin{cases} \dot{x}_{i,1}(t) = x_{i,2}(t) \\ \dot{x}_{i,2}(t) = f_i(.) + b_i(q)\,u_i(t), \\ \dot{x}_{i,3}(t) = \dot{f}_i(q,\dot{q},x_o) \end{cases} \tag{54}$$

Table 1 TMUBOT physical and mechanical features

Body Length	88	cm	Body Height From the Ground (with proper default angles)	50	cm	Exterior Offset of the Hip	7	cm
Body Width	24	cm	Body Weight	35	kg	Hip Length	34	cm
Body Height	14	cm	Approximate Portable Weight	10	kg	Knee Length	30.5	cm

where, $x_{i,3}$ is the extended state of i^{th} sub-system which represents all of theapplied internal and external disturbances to each sub-system. Actually, Eq. 53 is the general state space form of a quadruped robot and for tracking a predefined gate e.g., walk or trot, $x_{i,1}(t)\, x_{i,2}(t)$ should track their desired values $r_{i,1}(t)$, $\dot{r}_{i,1}(t)$ respectively, where $r_{i,1}(t)$ is the desired angular position and $\dot{r}_{i,1}(t)$ is the desired angular velocity of the related joint. According to Eq. 4, a TESO is designed for Eq. 54 in order to estimate and compensate the lumped disturbance and state vectors simultaneously, as follow:

$$\begin{cases} \dot{\hat{x}}_{i,1}(t) = \hat{x}_{i,2}(t) + \beta_{i,1}(t)\, e_{i,1}(t) \\ \dot{\hat{x}}_{i,2}(t) = \hat{x}_{i,3}(t) + \beta_{i,2}(t)\, e_{i,1}(t) + \hat{b}_i(q)\, u_i(t) \\ \dot{\hat{x}}_{i,3}(t) = \beta_{i,3}(t) e_{i,1}(t) \end{cases}, \quad (55)$$

where $\hat{x}_{i,j}$ is the estimated value of $x_{i,j}$, $e_{i,j}(t) = x_{i,j}(t) - \hat{x}_{i,j}(t)$ is the estimation error and $\beta_{i,j}(t) j = 123$ are the observer parameters. Also, the control input of each sub-system is designed as follows:

$$u_i(t) = \frac{1}{\hat{b}_i(q)}(-\hat{f}_i(q,\dot{q}) + \bar{u}_i(t)), \quad (56)$$

where in Eq. 56, $\bar{u}_i(t) = k_{i,1}\left(r_i(t) - \hat{x}_{i,1}(t)\right) + k_{i,2}\left(\dot{r}_i(t) - \dot{\hat{x}}_{i,2}(t)\right) + \ddot{r}_i(t)$ is a PD controller and $k_{i,1}$, $k_{i,2}$ are the design parameters. If $\beta_{i,j}(t)$ is designed so that $e_{i,j}(t) = 0$, then $x_{i,j} \cong \hat{x}_{i,j}$, $\hat{b}_i(\hat{q}) \approx b_i(q)$. Therefore, the closed loop system will be as follows:

$$\begin{cases} \dot{x}_{i,1} = x_{i,2} \\ \dot{x}_{i,2} = f_i(q,\dot{q}) + b_i(q_i)\left(\frac{1}{\hat{b}_i(\hat{q})}\left(-\hat{f}_i(q,\dot{q}) + \bar{u}_i(t)\right)\right) = \bar{u}_i(t) \end{cases}. \quad (57)$$

To wrap it, for each active joint of the TMUBOT a TESO and a PD controller have been designed according to Eqs. 55, 56 respectively. The considered structure is shown in Fig. 3. Simulation of the plant (TMUBOT) and the proposed algorithm have been performed in MSC ADAMS software and the ground is modeled with the assumed friction coefficient $\mu = 0.8$, in order to avoid slipping (see Fig. 4). According to the inverse kinematics of the robot, the gait planer is designed in such a way to produce the desired angular positions for a normal walking of the robot on the ground. For instance, Fig. 5 shows the desired angles of the joints for a walking locomotion. By proper tracking of the gait planar signals, the physical stability of the robot is guaranteed.

The first step is designing the TESO parameters$l_i(t)$. For this purpose, based on the previous section, the PD eigenvalues $\rho_i(t)$ are considered as:

$$\rho_{i,j}(t) = \bar{\rho}_{i,j}\omega_{i,ob}(t), i = 1, \ldots, 12, j = 1, 2, 3, \quad (58)$$

where $\omega_{i,ob}(t)$ is the TESO bandwidth, $\overline{\rho}_{i,1} = -\omega_0$, $\overline{\rho}_{i,2} = \omega_0(-\xi + j\sqrt{1-\xi^2})$ and $\overline{\rho}_{i,3} = \omega_0(-\xi - j\sqrt{1-\xi^2})$ are the roots of considered filters. Also,$\omega_0 = 1\xi = 0.707$ and the tuning of TESO parameters has done using Theorem 2. As it has been mentioned before, one of the significant parts of TESO is the time-varying bandwidth $\omega_{i,ob}(t)$. To form the observer bandwidth based on Theorems 1 and 2, the relation between $\omega_{i,ob}$ with κ, γ, η and δ should be analyzed. Therefore, the lumped disturbances that applied to each of the robot's joints must be examined. Figure 6 shows the lumped disturbance torques that applied to the first

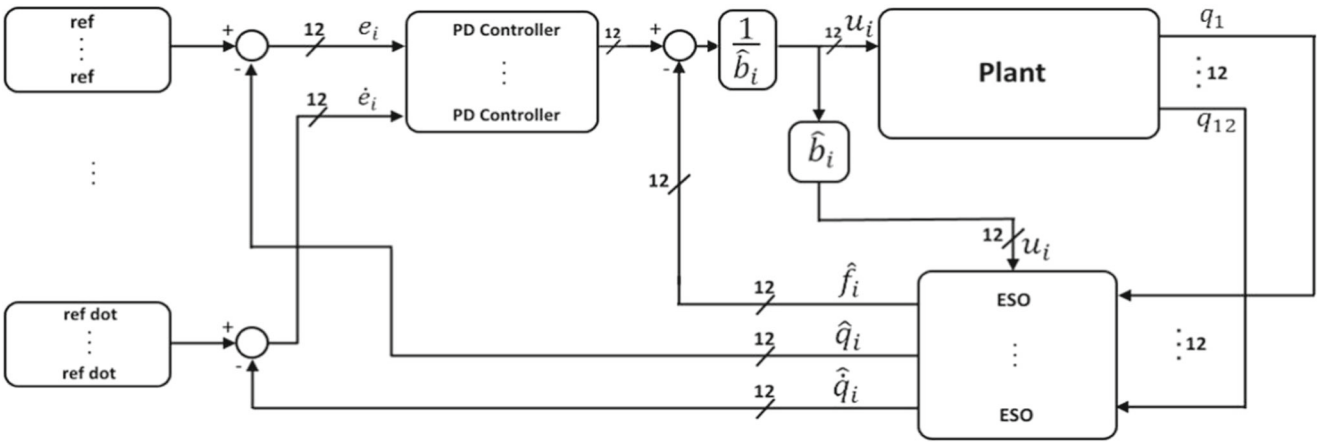

Fig. 3 The decentralized structure of TESO and PD controller that used for TMUBOT

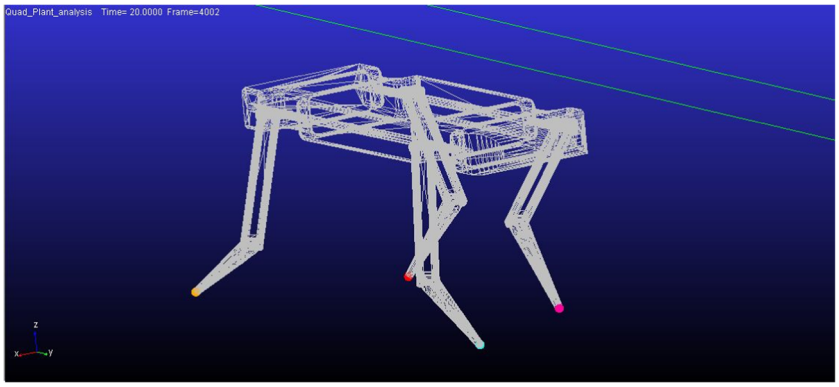

Fig. 4 Dynamic Simulation of TMUBOT in MSC ADAMS Environment

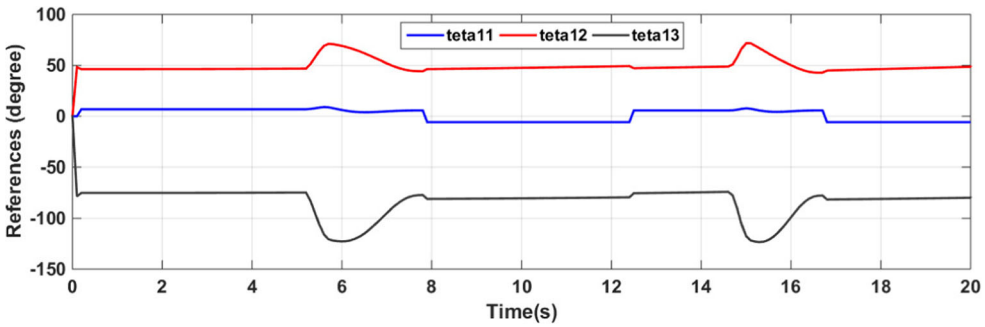

Fig. 5 Desired angular positions for walking locomotion

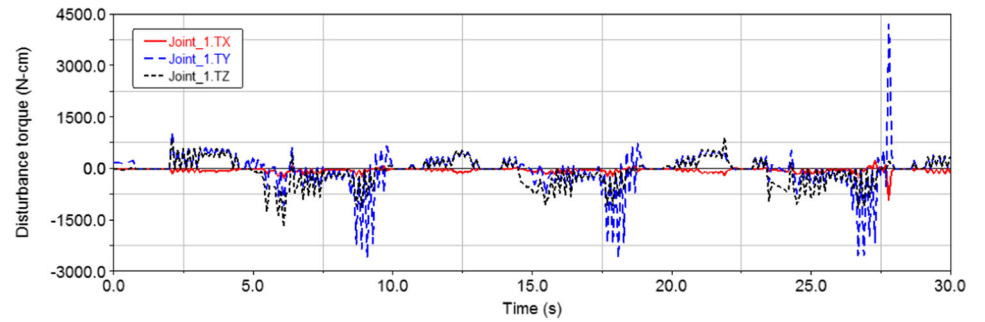

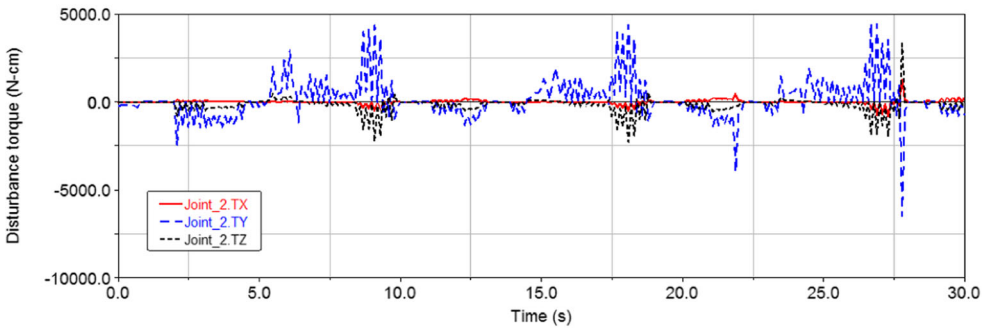

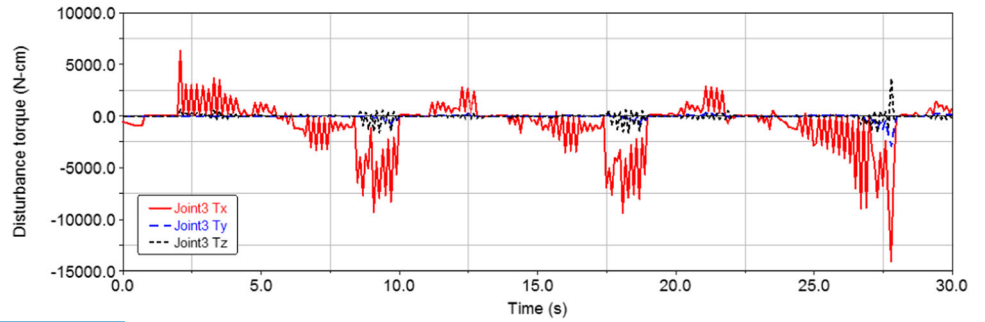

Fig. 6 Lumped disturbance torques that applied to the joints in three axis for Leg 1

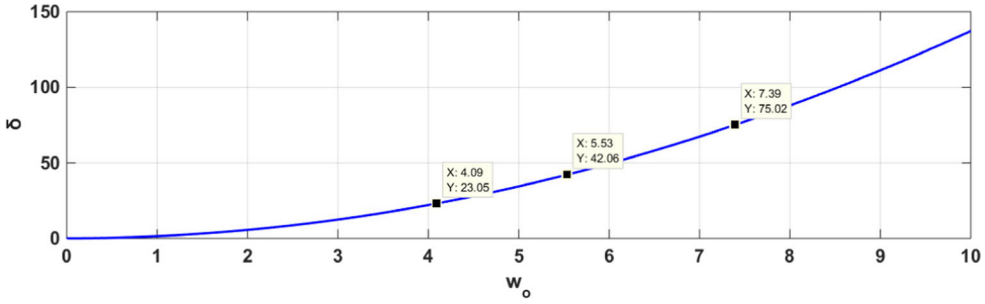

Fig. 7 The upper bound deviation of each joint in terms of the observer bandwidth

leg joints of the robot (Since there is a similarity between the robot legs, therefore the results of a single leg have presented). According to Fig. 6, the following relations on the norms of the lumped disturbance torques for each of the joints are obtained:

$$\begin{aligned} \|-b_1 h_1(x,w)\|_\infty &\le 25, \\ \|-b_2 h_2(x,w)\|_\infty &\le 45, \\ \|-b_3 h_3(x,w)\|_\infty &\le 75 \end{aligned} \tag{59}$$

Due to the disturbance bounds applied to each of the joints, design of the observer bandwidth should happen in a way that (59) holds at all times. By using (42), the upper bound deviation of each joint perturbed term in the observer bandwidth for the assumed eigenvalues is shown in Fig. 7. It is necessary to point out that, there is an inverse relationship between the observer performance in the estimation and the amount of lumped disturbance. According to Fig. 7, the minimum value of $\omega_{1,ob}$ in order to satisfy (59) for all of the joints are 4.09, 5.53 and 7.39 respectively. Moreover, according to Eq. 44, the deviations of estimation error envelope parameters on transient and steady-state response in terms of the observer bandwidth have been shown in Fig. 8. In order to have a desirable estimation, it is necessary for the gain of the transient response of the estimation error to be minimized and for its convergence rate to be maximized. Also, the steady state response of the estimation error converges to its minimum value over time. Thus, the initial value of the observer bandwidth should equal to the lowest value to satisfy the condition (42) or (59) and the final value of the observer bandwidth, should be considered according to the least steady state value possible for the bandwidth of each of the joints, and calculated as follows:

$$\omega_{ob_1}(t) = \begin{cases} 2.1, & t \le 0.5 \\ 8, & t > 0.5 \end{cases}, \tag{60}$$

$$\omega_{ob_2}(t) = \begin{cases} 2.1, & t \le 0.5 \\ 8, & t > 0.5 \end{cases}, \tag{61}$$

$$\omega_{ob_3}(t) = \begin{cases} 4.1, & t \le 0.5 \\ 8, & t > 0.5 \end{cases} \tag{62}$$

It is essential to note that an excessive increase in the observer bandwidth causes the estimation of angular velocity to have high volatility which causes instability of the closed-loop system. Also, it is an indisputable fact that there is a tradeoff between the gain of the transient response and the convergence rate of the estimation error envelope. This sequence repeats for other robot legs and

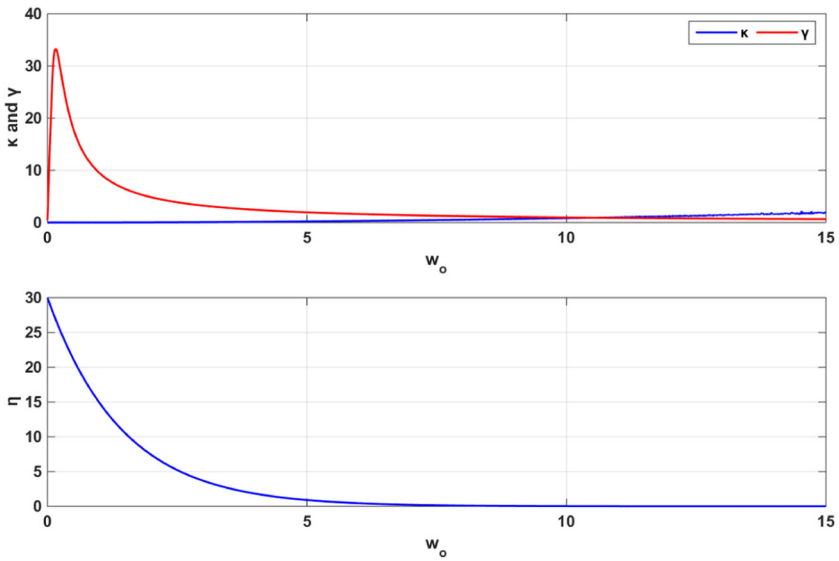

Fig. 8 Deviations of estimation error envelope parameters on transient and steady-state response in terms of the observer bandwidth

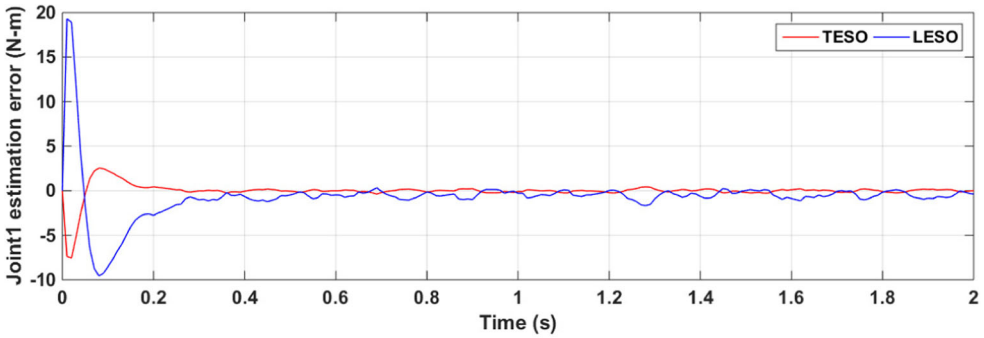

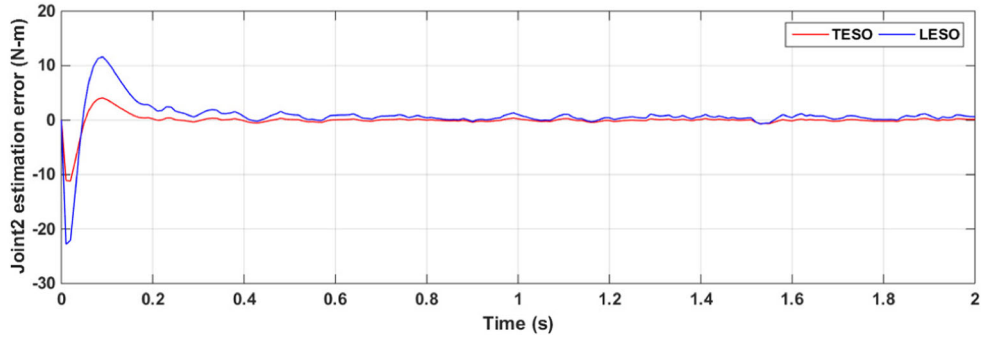

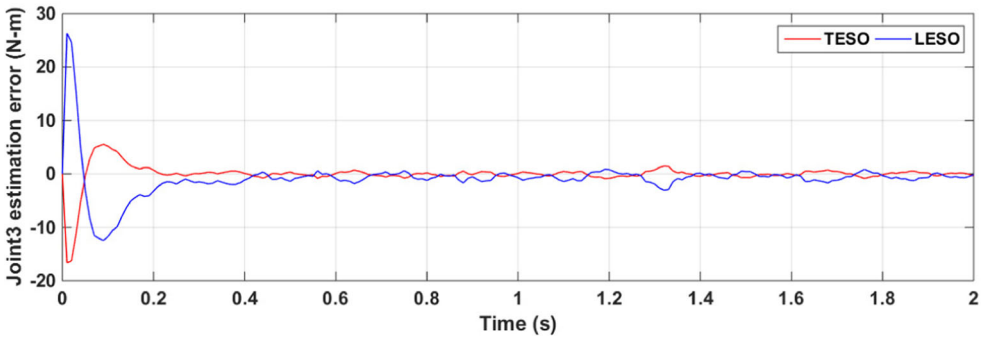

Fig. 9 Lumped disturbances estimation errors

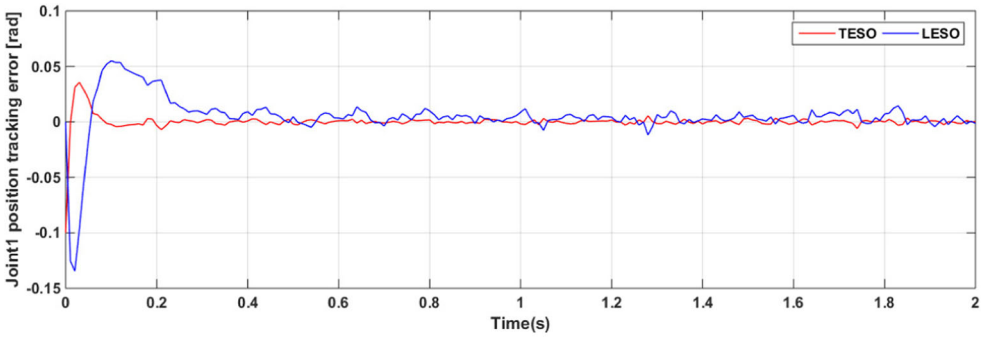

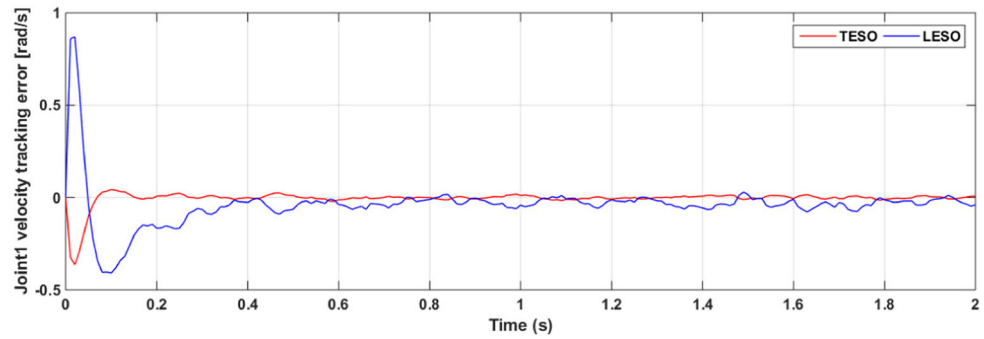

Fig. 10 Position and velocity tracking errors of Joint 1

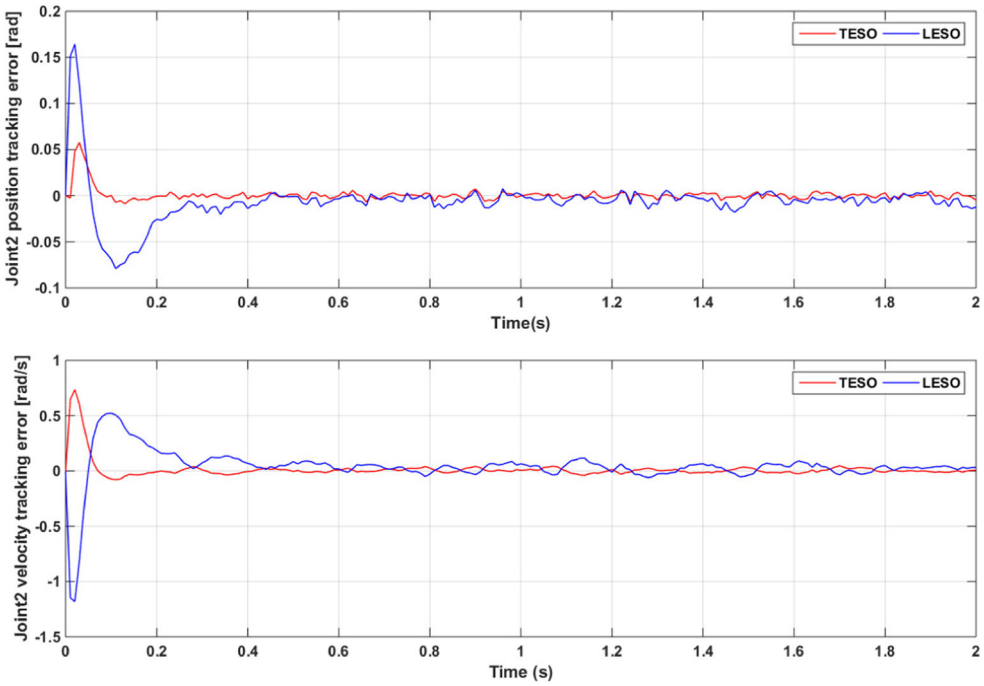

Fig. 11 Position and velocity tracking errors of Joint 2

the PD eigenvalues of each joint are calculated by finding the time shaping of the observer bandwidth and substituting ω_{ob_i} in Eq. 58. Then the coefficients $a_i(t)$ are calculated in terms of $\rho_i(t)$ by using the Eq. 27. Finally, in order to calculate the observer coefficients$l_i(t)$, Eq. 14 is used. In order to clarify the better performance of the time varying extended state observer, a linear extended state observer with time-invariant parameters has been designed for each of the robot joints, and the results of the two observers have been compared together. Figure 9 shows the lumped disturbance estimation errors of leg joints. According to Fig. 9 the primary overshoot in the estimation error signal of the time-varying extended state observer (the red graphs), has been desirably reduced compared to the linear extended state observer (the blue graphs). Moreover, the settling time of the estimation error signal in the time-varying extended

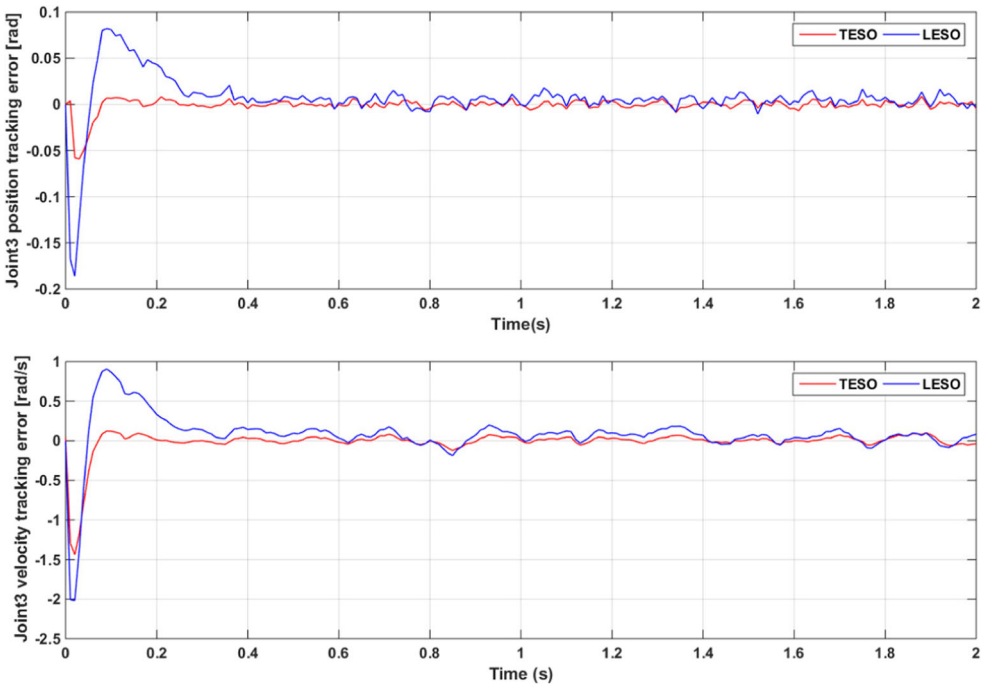

Fig. 12 Position and velocity tracking errors for Joint 3

state observer is less than the time for the linear extended state observer, which results in faster convergence in the closed loop response of the system in each time interval. This is due to the design ofω_{ob}, which is small at first, and increases with time. For tracking the desired gate, a proportional-derivative controller has been designed for each joint, as follows:

$$u_i = k_{i1}\left(r_{i1} - \hat{x}_{i1}\right) + k_{i2}\left(\dot{r}_{i1} - \hat{x}_{i2}\right) + \ddot{r}_{i1} i = 1 \ldots 12. \quad (63)$$

In Eq. 63, k_{i1} and k_{i2} are the coefficients of the proportional-derivative controller, r_{i1}, $\dot{r}_{i1}$, and $\ddot{r}_{i1}$ represent the desired angular position, velocity and acceleration, respectively. Furthermore,$\hat{x}_{i1}$ and $\hat{x}_{i2}$ denote the estimations of angular position and angular velocity, respectively. The estimation error of the angular position and angular velocity for each of the robot joints of a leg, are shown in Figs. 10, 11 and 12. Also, Figs. 13 and 14 show the control signals that applied to each leg joint by LESO and TESO respectively. According to Figs. 10, 11 and 12, the overshoot of the tracking errors in TESO structure are much less than LESO. Therefore, the actuators of the system need less torque for the desired tracking. Consequently, the cooperative work of TESO and PD controller results in more energy saving. Moreover, the settling time of tracking error is better when using TESO-based control, compared to previous methods (LESO algorithm), due to the fact that it provides better stability in the robot movement process, especially when an external force is applied to the system. It should be noted that for having a highly precise estimation of the states using the LESO algorithm, it is required to choose large parameters, which usually cause saturation in the actuators of the system, while this can be avoided when using TESO algorithm.

4.2 Implementation Results

The aim of this part is to present a practical verification of the proposed algorithm to control a complicated system without a precise model. According to Eq. 52 the term, $f_i(q\dot{q}x_o)$ includes all internal and external disturbances. The disturbances include forces that measuring them is not feasible or require expensive and high-resolution sensors. They include the coupling forces, ground reaction forces, friction forces. Whereas by using TESO algorithm, these physical variables can be estimated and compensated from the dynamic equations. As mentioned before, in this paper, a quadrupedal robot is used to examine the performance of the proposed algorithm. Each joint of TMUBOT is equipped with a brushless DC motor as the actuator of the system and the control signals are applied to the motors through

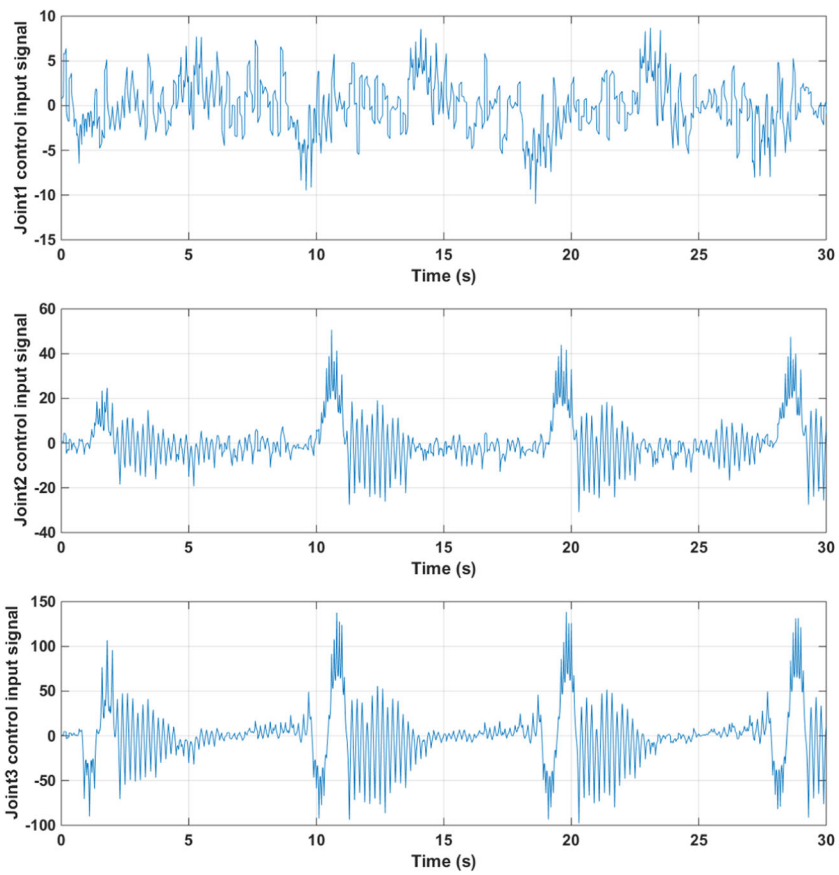

Fig. 13 Control signals applied to the leg joints by using LESO

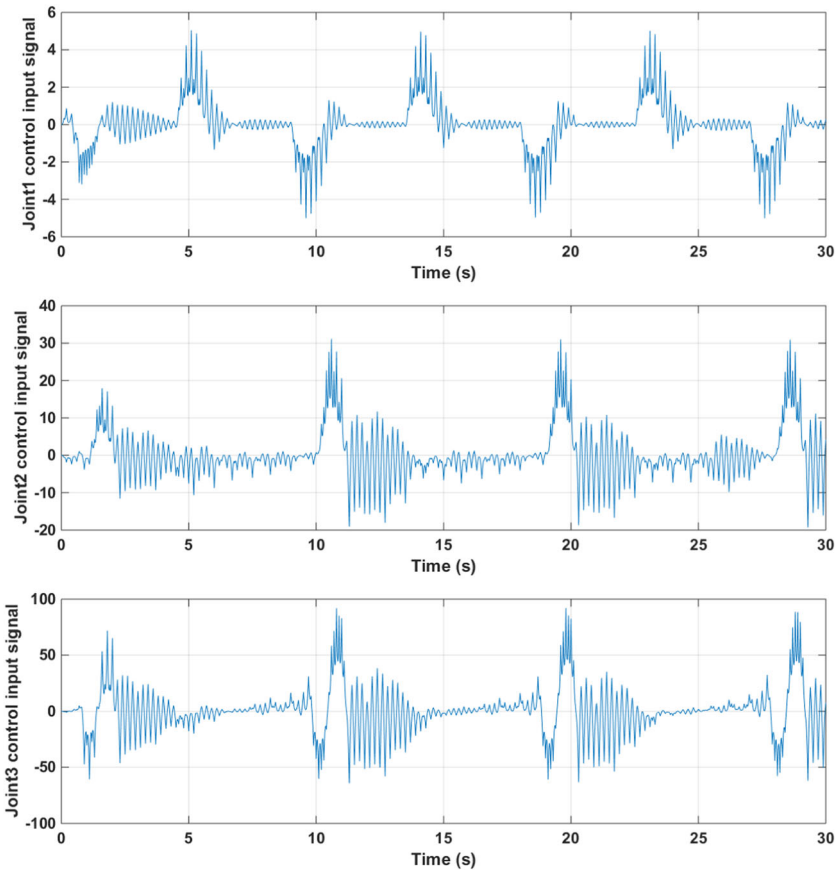

Fig. 14 Control signals applied to the leg joints by using TESO

EPOS2 drivers. Each joint has an encoder for measuring the actual angular position and velocity to update the TESO variable states and calculate the tracking error for the PD controller. To evaluate the performance of TESO algorithm, for each joint of TMUBOT, according to Eqs. 55, 63, a TESO and decentralized PD controller have been designed. The obtained results were compared with the most prevalent method, LESO algorithm, which is usually

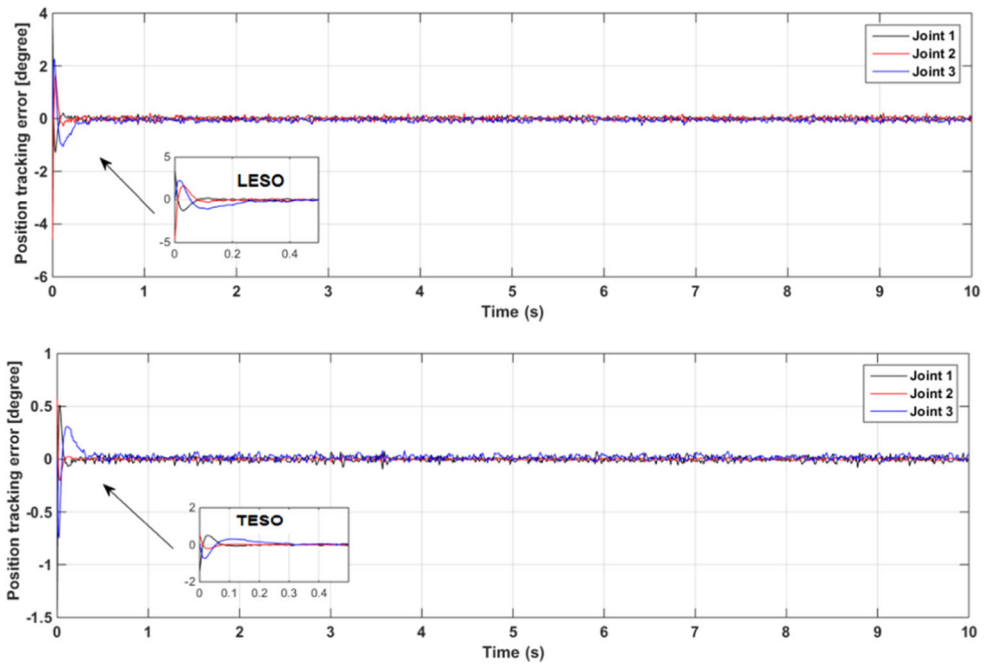

Fig. 15 Position tracking errors - Up: LESO and PD controller. Down: TESO with PD controller

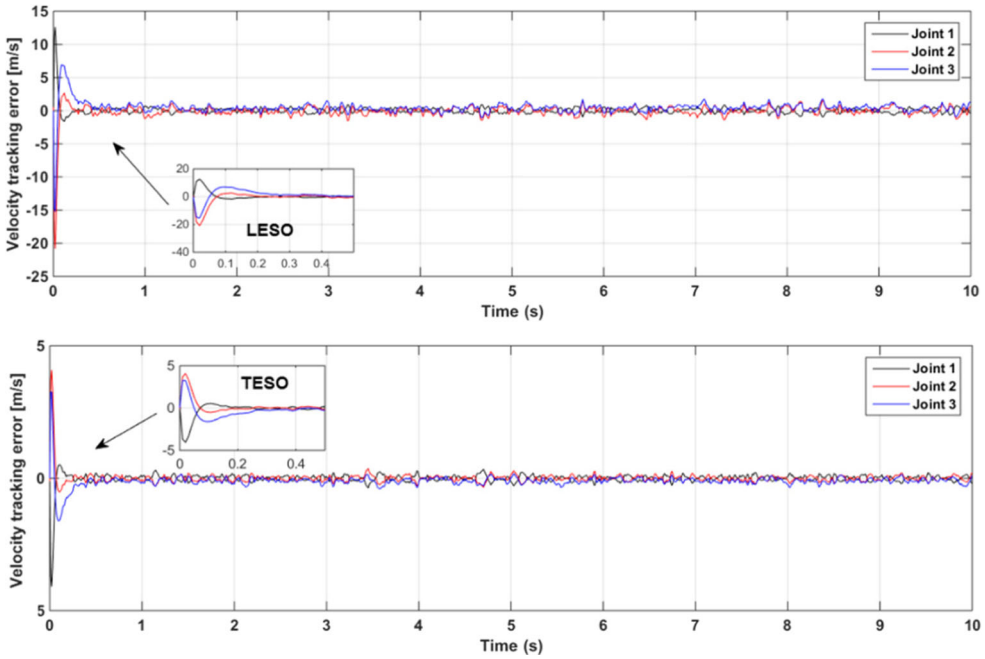

Fig. 16 Velocity tracking errors - Up: LESO and PD controller. Down: TESO with PD controller

used in practical schemes. To have a reasonable comparison between the performances of observers, the same control algorithms (PD Controller) have been designed for each observer. Figures 15 and 16, show the position and velocity tracking errors of a leg's joints of the robot by using the LESO and TESO. According to Figs. 15 and 16, the overshoot of position and velocity tracking errors in the TESO algorithm is remarkably less than those of the LESO algorithm. Furthermore, the settling times of both position and velocity tracking error through TESO algorithm are less than those of the LESO algorithm. In the LESO algorithm, to have a sustainable movement for the robot in the experiment, large parameters have been considered. Hence, the difference between the settling times is not substantial. Figure 17, shows the control signals of the LESO and TESO algorithms. According to Fig. 17, the control signals of actuators applied to joints through the TESO algorithm are much smaller than those of the LESO algorithm. Consequently, for the same trajectory, the TESO algorithm needs less torque compared to LESO, and this

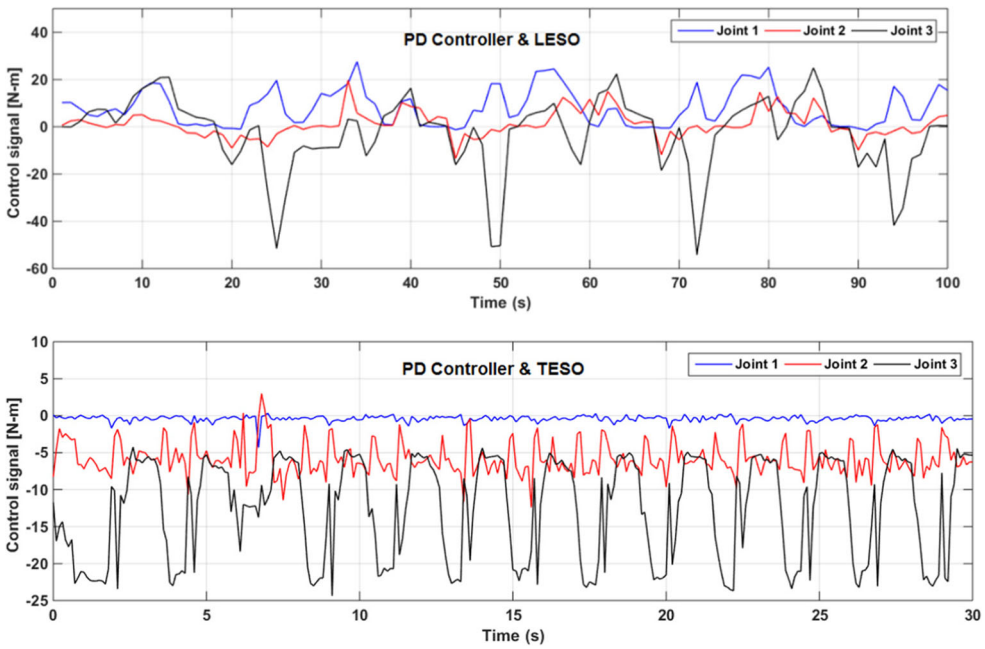

Fig. 17 Control signals - Up: LESO and PD controller. Down: TESO with PD controller

leads to less energy consumption. Whereas, it is likely for the control signal to pass the actuator saturation boundary when using the LESO algorithm.

5 Conclusions and Future Work

Finding a way to control systems without having precise information about their dynamics has been a challenge for control engineers. In this study, TESO is proposed to solve this problem. Boundedness of the estimation error dynamics is an important subject in the evaluation of observer design. Here, boundedness of the TESO estimation error dynamics is proved by means of DAST and spectral Lyapunov function. As a result, a design procedure for the TESO parameters has been achieved. According to the theorems presented here, the PD eigenvalues or the time-varying bandwidth ($\omega_{ob}(t)$) of the TESO estimation error as designing parameters, have relationships with the envelope parameters (gain, convergence rate and final value) of the TESO estimation error. Actually, the proposed theorems in this study, not only guarantee the stability of the TESO estimation error with the help of DAST, but also determined the relationship between the TESO design parameters and estimation error upper bound of the proposed observer. Therefore, by means of these relationship criteria such as overshoot and settling time can systematically be improved as much as possible. In order to evaluate the performance of the proposed method and also illustrate practical aspects of it, the TMUBOT quadruped robot has been used as an experimental application and a TESO with a PD controller has been applied to the system. The results show improvements in the estimation of internal and external disturbance by using TESO than previous methods like LESO. Actually, designing time-varying observer parameters yields better results than that of time-invariant one. Furthermore, TESO-based control structure has shown better performance in the estimation, in terms of transient and steady-state response, compared to the previous algorithms, e.g., LESO-based control structure. In future developments, considering frequency analysis in the design of observer bandwidth and applying other types of controllers with stability analysis is suggested in order to provide an even better performance. Moreover, by implementing the proposed theorems in diverse scenarios, e.g. applying an external force to the robot from the environment or using TESO based control in other industrial systems, the performance of the proposed method could be proved.

References

1. Chen, W.-H., Yang, J., Guo, L., Li, S.: Disturbance observer-based control and related methods—an overview. IEEE Trans. Ind. Electron. **63**, 2 (2016)
2. Sariyildiz, E., Ohnishi, K.: Stability and robustness of disturbance observer-based motion control systems. IEEE Trans. Ind. Electron. **62**(1), 414–422 (2015)
3. Besancon, G.: Nonlinear Observers and Applications. Springer, New York (2007)
4. Nozaki, T., Mizoguchi, T., Ohnishi, K.: Decoupling strategy for position and force control based on modal space disturbance observer. IEEE Trans. Ind. Electron. **61**(2), 1022–1032 (2014)
5. Huang, Y., Xue, W.: Active disturbance rejection control: Methodology and theoretical analysis. ISA Trans. **53**(4), 963–976 (2014)
6. Han, J.: A class of extended state observers for uncertain systems. Control Decis. **10**(1), 85–88 (1995)
7. Han, J.: From PID to active disturbance rejection control. IEEE Trans. Ind. Electron. **56**(3), 900–906 (2009)
8. Leonard, F., Martini, A., Abba, G.: Robust nonlinear controls of model-scale helicopters under lateral and vertical wind gusts. IEEE Trans. Control Syst. Technol. **20**(1), 154–163 (2012)
9. Gao, Z.: From linear to nonlinear control means: A practical progression. ISA Trans. **41**(2), 177–189 (2002)
10. Yao, J., Jiao, Z., Ma, D.: Extended-state-observer-based output feedback nonlinear robust control of hydraulic systems with back stepping. IEEE Trans. Ind. Electron. **61**(11), 6285–6293 (2014)
11. Attar, M., Majd, V.J., Dini, N., Edrisi, F.: Estimation of decenteralized unknown dynamics for a 2DOF manipulator using a time varying extended state observer. In: 4th International Conference on Robotics and Mechatronics (ICROM) (2016)
12. Yoo, D., Yau, S., Gao, Z.: Optimal fast tracking observer bandwidth of the linear extended state observer. Int. J. Control **80**(1), 102–111 (2007)
13. Zheng, Q., Gao, L.Q., Gao, Z.: On stability analysis of active disturbance rejection control for nonlinear time-varying plants with unknown dynamics. In: Proc. 46th Conf. Decision Control, pp. 3501–3506. New Orleans (2007)
14. Madoński, R., Herman, P.: Survey on methods of increasing the efficiency of extended state disturbance observers. ISA Trans. **6**, 18–27 (2015)
15. Gao, Z., Huang, Y., Han, J.: An alternative paradigm for control systems design. In: Proceedings of the 40th IEEE Conference on Decision and Control (2001)
16. Huang, Y., Xue, W.: Active disturbance rejection control: Methodology and theorical analysis. ISA Trans. **53**, 963–976 (2014)
17. Przybyla, M., Kordasz, M., Madoński, R., Herman, P., Sauer, P.: Active disturbance rejection control of a 2DOF manipulator with significant modeling uncertainty. Bull. Polish Acad. Sci. **60**, 3 (2012)
18. Khalil, H.K. Nonlinear Systems, 3rd edn., pp. 610–625. Englewood Cliffs, Prentice-Hall (2002)
19. Guo, B., Zhao, Z.: On the convergence of an extended state observer for nonlinear systems with uncertainty. Syst. Control Lett. **60**(6), 420–430 (2011)
20. Han, J., Zhang, R.: Error analysis of the second order ESO. J. Syst. Sci. Math. Sci. **19**(4), 465–471 (1999)
21. Guo, B., Zhao, Z.: On convergence of nonlinear active disturbance rejection for SISO systems. In: Control and Decision Conference the 24th. Taiyuan (2012)
22. Guo, B., Zhao, Z.: On convergence of nonlinear extended state observer for multi-input multi-output systems with uncertainty. IET Control Theory Appl. **6**(15), 2375–2386 (2012)

23. Zhao, Z.L., Guo, B.Z.: On active disturbance rejection control for nonlinear systems using time-varying gain. Eur. J. Control, 62–70 (2015)
24. Zhu, J.: A unified spectral theory for linear time-varying systems— progress and challenges. In: Proc. 34th Conf. Decision Control, pp. 2540–2546. New Orleans (1995)
25. Liu, Y., Zhu, J.: Regular perturbation analysis for trajectory linearization control. In: Proc. Amer. Control Conf., New York, pp. 3053–3058 (2007)
26. Jim Zhu, J., Liu, Y., Hang, R.: A spectral Lyapunov function for exponentially stable LTV systems. Amer. Control Conf., Hyatt Regency Riverfront (2009)
27. Silverman, L.M.: Transformation of time-variable systems to canonical (phase-variable) form. IEEE Trans. Autom. Control **11**(2), 300–303 (1966)
28. Farid, Y., Majd, V.J., Ehsani-Seresht, A.: Fractional-order active fault-tolerant force-position controller design for the legged robots using saturated actuator with unknown bias and gain degradation. Mech. Syst. Signal Process. **104**, 465–486 (2018)
29. Graham, A.: A note on a transformation between two canonical forms in state-space in terms of the eigenvalues of the system matrix. IEEE Trans. Autom. Control **13**(4), 448 (1968)
30. Wolovich, W.A.: On the stabilization of controllable systems. IEEE Trans. Autom. Control **13**(5), 569–572 (1968)
31. Edrisi, F., Majd, V.J., Attar, M., Dini, N.: Modifying the attitude of quadruped robot body against disturbances via data fusion. In: 2016 4th International Conference on Robotics and Mechatronics(ICROM), pp. 55–60. IEEE (2016)
32. Dini, N., Majd, V., Edrisi, F., Attar, M.: Estimation of external forces acting on the legs of a quadruped robot using two nonlinear disturbance observers. In: Proceedings of the 4th International Conference on Robotics and Mechatronics (ICROM), pp. 72–77, Tehran (2016)
33. Li, Z., Xiao, S., Sam, S., Su, H.: Constrained multi-legged robot system modeling and fuzzy control with uncertain kinematics and dynamics incorporating foot force optimization. IEEE Trans. Man Cybern. Syst. (2015)

Mehran Attar received his B.Sc. degree in Control Engineering in 2013 from Hamedan University of Technology, Hamedan Iran. During his studies for completing the BSc, He passed about two years at Sharif University of Technology as a temporary-transfer student. He received his MSc degree in 2017 from the control engineering department of Tarbiat Modares University (TMU), Tehran, Iran. He currently works with the research and development department of MAPNA group. His areas of interest include: Intelligent identification and control, multi-agent learning, robust nonlinear control, machine learning, modelling and control of robotic systems and wind turbines.

Vahid Johari Majd received his B.Sc. degree in 1989 from the electrical engineering department of the University of Tehran, Iran. He then received his M.Sc. and Ph.D. degrees in the area of Control Theory from the electrical engineering department of the University of Pittsburgh, PA, U.S.A. in 1991 and 1995, respectively. He is currently an associate professor in the control system department of Tarbiat Modares University, Tehran, Iran, and is the director of intelligent control systems laboratory. His areas of interest include: Intelligent identification and control, multi-agent learning, fuzzy control, cooperative control, formation control, robust nonlinear control, fractional order control, and robotic systems.

Navid Dini received his B.Sc. degree in 2009 from the electrical engineering department of Shahrood University of Technology, Semnan, Iran. He then received his M.Sc. degree in the area of Control Theory from the electrical engineering department of Amirkabir University of Technology, Tehran, Iran, in 2013. He is currently a PhD candidate in the control systems department of Tarbiat Modares University, Tehran, Iran. His areas of interest include: fuzzy control, intelligent identification and control, discrete event systems, model predictive control, and robotic systems.